RESEARCH ARTICLE

GCB-BIOENERGY
BIOPRODUCTS FOR A SUSTAINABLE BIOECONOMY WILEY

Multispectral image analysis detects differences in drought responses in novel seeded *Miscanthus sinensis* hybrids

Boris Lazarević[1,2] | Mislav Kontek[3] | Klaudija Carović-Stanko[2,4] |
John Clifton-Brown[5] | Mohamad Al Hassan[6] | Luisa M. Trindade[6] | Vanja Jurišić[3]

[1]Department of Plant Nutrition, University of Zagreb Faculty of Agriculture, Zagreb, Croatia

[2]Centre of Excellence for Biodiversity and Molecular Plant Breeding, Zagreb, Croatia

[3]Department of Agricultural Technology, Storage and Transport, University of Zagreb Faculty of Agriculture, Zagreb, Croatia

[4]Department of Seed Science and Technology, University of Zagreb Faculty of Agriculture, Zagreb, Croatia

[5]Institute of Biological, Environmental and Rural Sciences (IBERS), Aberystwyth University, Aberystwyth, UK

[6]Wageningen University & Research, Plant Breeding, Wageningen, The Netherlands

Correspondence
Mislav Kontek, Department of Agricultural Technology, Storage and Transport, University of Zagreb Faculty of Agriculture, Svetošimunska cesta 25, 10000 Zagreb, Croatia.
Email: mkontek@agr.hr

Abstract

Drought tolerance in *Miscanthus sinensis* is a desirable trait because of its potential use to develop new varieties, namely intra-specific hybrids, adapted to drought-prone marginal lands. In this study, drought tolerance was evaluated on 8 *M. sinensis* intra-specific hybrids (GRC1–GRC8). Plants were grown in the growth chamber (14/10 h, 25/20°C, 70% relative air humidity and $300\,\mu mol\,m^{-2}\,s^{-1}$ irradiance). Drought was induced by withholding irrigation for 21 days (stress phase) and after re-watering (recovery phase) for 7 days. Nondestructive multispectral 3D images for plant morphology, color, and chlorophyll fluorescence imaging were used to quantify drought-induced changes on a weekly basis for the entire duration of the experiment. Total leaf area (TLA) and digital biomass (DB) responded most rapidly to water deficits (7–14 days), followed by leaf senescence (14–21 days), and finally, a drop in the maximum efficiency of PSII (F_v/F_m; 21 days). Traits measured on the last day of the drought treatment were used to calculate the phenotypic plasticity. Significant differences in drought susceptibility and phenotypic plasticity were found among the studied hybrids. Drought treatment (21 days) reduced DB and TLA on average by 50%, normalized difference vegetation index (NDVI) by 20% and F_v/F_m from 0.79 (in control) to 0.69 in the less drought-susceptible hybrids (GRC4 and GRC5), whereas in drought-sensitive hybrids (GRC2 and GRC3), 21 days of drought reduced DB and TLA on average by 80%, NDVI by 45% and F_v/F_m dropped from 0.79 (in control) to 0.35. The more drought-resilient hybrids showed lower phenotypic plasticity than their more sensitive counterparts, a stay-green strategy enabled through lower

Abbreviations: ANOVA, analysis of variance; ARI, anthocyanin index; B, blue; CHI, chlorophyll index; DB, digital biomass; F_0, minimum chlorophyll fluorescence; F_m, maximum chlorophyll fluorescence; F_v/F_m, maximum efficiency of photosystem two; G, green; HUE, hue; K, kelvin; L, liter; LAI, leaf area index; LANG, leaf angle; LED, light-emitting diode; LINC, leaf inclination; LPD, light penetration depth; MT, measurement time; NDVI, Normalized Digital Vegetation Index; NIR, near-infrared; PAR, photosynthetically active radiation; PCA, principal component analysis; PH, plant height; PLA, projected leaf area; PS(II), photosystem two; PSII, photosystem two; PSRI, Plant Senescence Reflectance Index; R, reflectance; R_{Blue}, reflectance in blue; RDPI, relative distance plasticity index; R_{FarRed}, reflectance in far-red; R_{Green}, reflectance in green; RMT, recovery measurement time; R_{NIR}, reflectance in near-infrared; R_{Red}, reflectance in red; SAT, saturation; SE, standard error; TLA, total leaf area; UV, ultraviolet; VAL, value; VWC, volumetric water content.

---

biomass accumulation and by extension, reduced water usage. Multispectral imaging and image analysis enabled fast and nondestructive quantification of plant morphological and physiological responses under drought conditions and could be used as an effective screening tool for drought susceptibility.

KEYWORDS

drought, *Miscanthus sinensis*, multispectral analyses, phenotyping, recovery

1 | INTRODUCTION

Miscanthus is a leading perennial energy crop because of its high dry matter yield potential and ability to achieve it under a wide range of climatic conditions (Clifton-Brown et al., 2017; Lewandowski et al., 2018) but also because of its low requirements in terms of fertilizers, herbicides, and management (Clifton-Brown & Lewandowski, 2000; Lewandowski & Schmidt, 2006; Wagner et al., 2019). At present, in Europe, miscanthus is mostly used as a feedstock in electricity and heat generation and as a building material (Lewandowski et al., 2018; Wagner et al., 2019). Moreover, there are other applications in research focus, such as biogas production, conversion to second-generation biofuels, and biochemicals, including bioplastics. Those various utilization options allow a high-value application of miscanthus biomass (Lewandowski et al., 2018; Wagner et al., 2019).

However, using agricultural land for miscanthus production could conflict with food production and global food security policy. FAO's scenario project report (FAO, 2018) shows that feeding a world population of almost 10 billion people in 2050 would require raising overall food production by more than 54% from the base year of 2012. Such an increase in food production will require maximum utilization of all available agricultural land. Thus, an alternative strategy for energy crop production is to cultivate them on poor soils where the cultivation of food crops is not economically viable, also known as marginal lands (He et al., 2022; Scordia et al., 2022). There, the competition for the use of irrigatable land for the production of food versus fuel would be circumvented (Lewandowski et al., 2016). Miscanthus could have a crucial role in biomass production on marginal land because it displays remarkable adaptability to different environments (Donnison & Fraser, 2016; Kalinina et al., 2017). However, drought stress may regularly occur in the majority of miscanthus species production scenarios, especially on those involving the production on marginal soils (Jones et al., 2015; Quinn et al., 2015). The naturally occurring interspecies hybrid *M. × giganteus* imported from Japan (Greef & Deuter, 1993), currently being the most cultivated biomass crop from the genus *Miscanthus*

(*M. sacchariflorus × M. sinensis*) is relatively sensitive to drought. This is mainly due to its failure to regulate its rate of water loss during the onset of drought, rendering it susceptible to yield loss and death in severe and prolonged droughts (Clifton-Brown & Lewandowski, 2000). Sacks et al. (2013) suggested that it may be possible to increase drought tolerance through breeding with drought-tolerant parental genotypes and van der Weijde et al. (2017) identified *M. sinensis* genotypes that are more tolerant to drought. Long-term field trials showed that *M. sinensis* hybrids could achieve high yields under different climatic conditions (Gauder et al., 2012), adapt to a wide range of geographical conditions, and possess extensive genetic diversity (Gifford et al., 2015; Nie et al., 2017), which makes it a good candidate for the optimization of abiotic stress tolerance. Correspondingly, Clifton-Brown and Lewandowski (2000) reported that triploid *M. sinensis* hybrids could be more drought tolerant in comparison with *M. × giganteus* in controlled environments. Besides, they reported that *M. sinensis* retained the lowest leaf conductance and showed slower leaf senescence in water-deficit conditions in comparison with *M. × giganteus* and *M. sacchariflorus*, which indicates different drought response strategies among these species (Clifton-Brown & Lewandowski, 2000).

While experiencing drought, plants show several differential morphological and physiological responses, which help them in coping with stressful conditions (Osakabe et al., 2014; Tuberosa, 2012). The impact of environmental stimuli on the affected plants, exemplified in the changing morphophysiological traits, is known as phenotypic plasticity (Valladares et al., 2006). Correspondingly, the assessment of phenotypic plasticity under drought conditions may contribute to a better understanding of this stress' footprint and enable the identification of potential traits for optimized drought tolerance through classical breeding (Tuberosa, 2012).

Recently, sophisticated nondestructive phenotyping techniques have been developed to detect the physiological status of plants exposed to drought. Due to a wide range of plant traits affected by drought, a more integrative approach that will use multiple sensors and gain information about multiple phenotypic traits is needed. Nondestructive plant

imaging techniques such as chlorophyll fluorescence and multispectral imaging are based on the reflectance of different wavelengths from the plant leaves and are used for the calculation of different vegetation indices (VIs) as indicators of plant chemical composition and physiological status (Dhondt et al., 2013; Munns et al., 2010). Chlorophyll fluorescence imaging represents a powerful plant phenotyping tool, which provides information about the efficiency of photosynthetic apparatus and associated physiological processes (Dhondt et al., 2013; Humplik et al., 2015; Wang et al., 2018). Similar techniques were previously used in experiments with Miscanthus; high-throughput phenotyping techniques were used for screening biomass accumulation and water use of 47 miscanthus genotypes under water-deficit stress (Malinowska et al., 2017), and the biomass quality of three *Miscanthus* genotypes under the water-deficit and nutrient-deficit stress (da Costa et al., 2019), both showing the genotypic variability in phenotypic reaction to drought.

The objectives of this study were to use multispectral imaging and image analysis to (i) assess differences in drought responses among novel *M. sinensis* (Anderss.) hybrids, (ii) quantify changes in morphological and physiological traits, and (iii) determine the phenotypic plasticity among the studied panel of hybrids under drought.

2 | MATERIALS AND METHODS

2.1 | Plant material and experimental conditions

Eight novel *M. sinensis* (Anderss.) seed-based hybrids (further referred to as GRC1–GRC8) were used in this experiment. Hybrids were provided by the Wageningen University and Research (WUR), The Netherlands. Plants were provided as 8-week-old seedlings grown in plugs, which were transplanted to 2 L plastic pots filled with 600 g of KLASMANN TS 1 fine pot soil. Ten uniformly developed plants per hybrid were selected for the experiment after additional 14 days of adaptation and growth. During this period, plants were irrigated with half-strength Hoagland's nutrient solution (Hoagland & Arnon, 1950). The experiment was conducted in a climate-controlled growth chamber at the University of Zagreb Faculty of Agriculture, Croatia. The following conditions were used: photoperiod of 14/10 h, temperature fluctuating between 25 and 20°C, during day and night regimes, respectively, 70% relative air humidity and 300 μmol m^{-2} s^{-1} irradiance, which was enabled through a photosynthetically active radiation (PAR) provided by Valoya L35, NS12 spectrum LED lights (Valoya Oy).

Five plants per hybrid, used as biological replicates, were subjected to the drought treatment (D), by withstanding irrigation completely for 3 weeks, whereas five control (C) plants per hybrid were regularly irrigated to keep ~40% substrate volumetric water content (%VWC). Substrate VWC was monitored using a substrate-calibrated WET sensor, an HH2 Moisture Meter (Delta-T Devices Ltd.). Average values of measured VWC are shown in Figure S1. After 3 weeks, plants subjected to the drought treatment were irrigated, to a VWC of (~40%), equal to the control plants, for 1 week (duration of the post-drought recovery study).

The experiment was set up as a completely randomized design. Measurements were performed at the onset of drought treatment (MT0), once per week (a 7-day basis) during the 3 weeks of drought treatment (MT1, MT2, and MT3). Additional measurements were performed on plants from the drought treatment after 7 days of recovery (RMT).

3 | MEASUREMENTS

3.1 | Multispectral and chlorophyll fluorescence imaging

Table S2 contains a list of all measured traits and abbreviations, as well as the devices and software used in the analyses. CropReporter™ was used for chlorophyll fluorescence and multispectral imaging (PhenoVation B.V.). Detailed description of the CropReporter™ is given in Lazarević et al. (2021).

Chlorophyll fluorescence measurements were taken on plants that had been dark-adapted overnight (10 h). Red light-emitting diode (LED) at 4000 mol m^{-2} s^{-1} intensity was used as saturating pulse. The induction curve was captured in 20 frames (20 images per second in 1.3 Mp). Images of minimum chlorophyll fluorescence (F_0) and maximum chlorophyll fluorescence (F_m) were captured after 20 and 800 ms, respectively. F_0 and F_m were used to calculate the maximum efficiency of PSII (F_v/F_m; Schreiber et al., 1995).

Color and spectral reflectance (R) images were captured at 50% light intensity power, resulting in 250 mol m^{-2} s^{-1} produced by broadband white LEDs. Images were captured at different reflectance (R) wavelengths, R_{Red}—640 nm, R_{Green}—550 nm, R_{Blue}—475 nm, R_{Chl}—730 nm, R_{NIR}—769 nm, and R_{FarRed}—710 nm.

The chlorophyll index (CHI) and anthocyanin index (ARI) were calculated from reflectance images, with CHI $= (R_{700})^{-1}$ to $(R_{769})^{-1}$ (Gitelson et al., 2003) and ARI $= (R_{550})^{-1}$ to $(R_{700})^{-1}$ (Gitelson et al., 2001).

After converting R_{Red}, R_{Green}, and R_{Blue} to values 0–1, the hue (0–360°), saturation (SAT), and value (VAL) were calculated.

The following formula was used to calculate hue (0–360°):

$$\text{HUE} = 60 \times \left(0 + \left(R_{\text{Green}} - R_{\text{Blue}}\right)/(\max - \min)\right), \text{if } \max = R_{\text{Red}};$$

$$\text{HUE} = 60 \times \left(2 + \left(R_{\text{Blue}} - R_{\text{Red}}\right)/(\max - \min)\right), \text{if } \max = R_{\text{Green}};$$

$$\text{HUE} = 60 \times \left(4 + \left(R_{\text{Red}} - R_{\text{Green}}\right)/(\max - \min)\right) \text{ if } \max = R_{\text{Blue}}.$$

In the case of HUE 0, 360 was added.

Value (0–1) was calculated as follows: $\text{VAL} = (\max + \min)/2$; where max and min were chosen from the R_{Red}, R_{Green}, and R_{Blue}. Saturation (0–1) was calculated as follows: $\text{SAT} = (\max - \min)/(\max + \min)$ if $\text{VAL} > 0.5$, or $\text{SAT} = (\max - \min)/(2.0 - \max - \min)$ if VAL 0.5, where max and min were chosen from the R_{Red}, R_{Green}, and R_{Blue}. In the above equations, Max and Min denote maximal or minimal reflectance in red (R_{Red}), green (R_{Green}) or blue (R_{Blue}) spectrum, respectively.

Several CropReporter-obtained parameters are shown in Figure S3.

3.2 | Multispectral scanning in 3D

The PlantEye F500 multispectral 3D scanner was used to perform multispectral scanning (Phenospex). Using HortControl™ software, various morphological parameters and VIs were calculated from 3D plant models (Phenospex). Lazarević et al. (2021) provide a detailed description of the PlantEye, including the resolution and wavelengths for scanning, and the creation of the 3D plant model.

For a better understanding of the measured traits, we will briefly explain the calculation of each parameter in the following section.

3.2.1 | Vegetation indices

Greenness $(\text{GR}) = (2 \times R_{\text{Green}} - R_{\text{Red}} - R_{\text{Blue}})/(2 \times R_{\text{Red}} + R_{\text{Green}} + R_{\text{Blue}})$.

Normalized Differential Vegetation Index $(\text{NDVI}) = (R_{\text{NIR}} - R_{\text{Red}})/(R_{\text{NIR}} + R_{\text{Red}}$; Rouse et al., 1974).

Plant Senescence Reflectance Index (PSRI) $\text{PSRI} = (R_{\text{Red}} - R_{\text{Gren}})/(R_{\text{NIR}}$; Merzlyak et al., 1999).

3.2.2 | Morphological parameters

Plant height (PH; mm) is calculated as a z-axis distribution of elementary triangles.

Leaf area projected (LAP; cm^2) is calculated as the area of all elementary triangle projections on the X–Y plane.

Total leaf area (TLA; cm^2) is calculated as the sum of all triangle domains, where each domain represents a group of triangles forming a uniform surface.

Digital biomass (DB; cm^3) is calculated as PH and 3D leaf area.

Leaf area index (LAI, mm^2 mm^{-2}) is calculated as TLA/sector size.

Leaf inclination (LINC; mm^2 mm^{-2}) is calculated as TLA/LAP.

The leaf angle (LANG; °) is the angle between the leaf blade and the main stem.

The deepest point through which the laser can penetrate the canopy is used to calculate light penetration depth (LPD; mm).

Figure S4 shows a selection of traits obtained by PlantEye.

3.3 | Phenotypic plasticity

Phenotypic plasticity for each hybrid was estimated by calculating the relative distance plasticity index (RDPI) for all morphological and physiological traits measured at MT3. RDPI represents the relative phenotypic distance between individuals of the same hybrid exposed to different treatments (C and D; Valladares et al., 2006). RDPI was calculated according to Valladares et al. (2006), and its values range from 0 to 1. Briefly, for each hybrid (GRC1–GRC8) and each trait (x), a rectangular matrix ($i \times j$) was created; rows (i) represented two treatments (D and C), and columns (j) represented five individuals (plants/replicates of each hybrid per treatment). For a given trait x, the distance among values ($d_{ij} \rightarrow_{ij'}$) is calculated as the difference $x_{i'j} - x_{ij}$. Thus, the absolute distance was calculated as pairwise differences for all traits across all individuals of each hybrid. Then, relative distances ($\text{rd}_{ij} \rightarrow_{ij'}$) which are defined as $d_{ij} \rightarrow_{ij'}/(x_{ij'} + x_{ij})$ for all pairs of individuals were calculated, and finally, RDPIs were calculated as $\Sigma(\text{rd}_{ij} \rightarrow_{ij'})/n$, where n represents the number of distances.

3.4 | Statistical analysis

Data were analyzed using SAS for Windows 9.3 (SAS Institute Inc., 2011). Before the statistical analysis, normality was tested by the Shapiro–Wilk test and homoscedasticity by assessing the plot of residuals against fitted values.

Repeated measures in Proc mixed, with hybrids ($n = 8$) and treatments ($n = 2$) as fixed effects, plant number ($n = 5$) as subject and measurement time (MT) as the

repeated measurement were performed for testing the difference among hybrids, treatments, and their interactions. The covariance was modelled according to the residual log-likelihood and Akaike's information criterion. In the case F test was significant, multiple comparison procedure was performed, and pairwise differences were computed for fixed effects and their interactions using the Tukey's HSD test ($p \leq 0.05$). The differences between hybrids and treatments (drought treatment and recovery) were evaluated with a two-way analysis of variance (ANOVA). By contrast, the differences in RDPI were evaluated with one-way ANOVA, followed by the post-hoc Tukey's HSD mean comparison test ($p \leq 0.05$).

The selected traits are presented as figures, means ± standard errors (SE), and the rest of the data (traits), along with the ANOVA tables, are given as Supplementary Tables.

Pearson's correlation coefficients were calculated and tested using the CORR procedure. A principal component analysis (PCA) was performed for all measured traits at MT3, using all experimental plants (two treatments × eight hybrids × five plants = 80). The first two principal components (PCs) were used to construct a biplot.

4 | RESULTS

Eight *M. sinensis* hybrids (GRC1–GRC8) were grown in control (40% VWC) and drought conditions, the latter was set up by the complete omission of irrigation for 21 days. Average values of soil VWC decreased from 45% at MT0 to 8.5% at MT3 (Figure S1) in the pots of the water stress plants. After 21 days, plants from the drought treatment underwent a short period of post-stress recovery, by reinstating irrigation (increasing and maintaining soil VWC at 40%) for 7 days.

4.1 | Morphology-related traits during drought and recovery

Multispectral scanning resulted in 3D cloud points from which 3D plant models were created (examples in Figure S4) and used for morphological analysis. In control treatment highest DB, PH and leaf area–related traits were found for GRC3 followed by GRC2 and GRC1. Drought treatment significantly reduced DB, TLA, LAP, and LAI at MT2 for GRC1, GRC2 and GRC3, and MT3 for all hybrids (Figures 1 and 2; Table S6). Drought treatment affected the average PH and LPD after MT2 for all hybrids. However, a significant reduction in average PH and LPD was reported only for GRC1, GRC2, and GRC3 at MT3 (Table S6).

Average LANG significantly increased in control and decreased in drought treatment over the applied stress timeline (MT0–MT3), and the opposite was true for LINC. Significant differences in average LANG and LINC between D and C plants were found at MT3 (Tables S5 and S6).

After 7 days of recovery, a significant increase in average DB, TLA, LAP, and LAI was determined; meanwhile, there was no significant ($p > 0.05$) change in PH, LPD, LANG, and LINC. The highest increase in DB, TLA, LAP, and LAI was observed for GRC1 and GRC5, and the lowest for GRC2 and GRC3 (Figure 3; Table S7).

4.2 | Color traits during drought and recovery

Plant color analysis was performed by measuring reflectance in red (R_{Red}), green (R_{Green}), and blue (R_{Blue}). In addition, an alternative way for color analysis by calculation of hue (HUE), saturation (SAT), and value (VAL) was used. HUE considers the ratio between reflectance in red, green, and blue, VAL represents lightness or darkness of the color, and the SAT is the intensity of color.

Drought affected all measured color traits, and most sensitive to drought were R_{Blue} and SAT. Namely, drought increased average R_{Blue} and decreased average SAT at MT2, whereas all other color traits were affected at MT3 (Table S6). For both control and drought, an increase in R_{Red}, and R_{Blue} was reported from MT0 to MT3, although this increment was more pronounced in drought plants. At MT3 significant differences between D and C plants in R_{Red} were found for GRC3 and GRC8 and in R_{Blue} for GRC1, GRC2, GRC3, GRC7, and GRC8. In both C and D plants, R_{Green} reported a drop in the period between MT0 and MT1, before increasing in C plants, and was constant for D plants. Significant differences in average R_{Green} between C and D plants were found at MT3 (Table S6).

HUE increased for both D and C plants from MT0 to MT1 and decreased for D plants at MT3. At MT3 significantly higher HUE for C compared with D plants were found for GRC2, GRC3, GRC6, GRC7, and GRC8 (Figure 4; Table S6). In addition, at MT3 there was no difference in HUE among hybrids grown in control, however in drought treatment, higher HUE values were found for GRC1, GRC4, and GRC5 compared with GRC2, GRC3, and GRC8. VAL decreased from MT0 to MT1 and then increased at MT3, which was more pronounced for control plants. Drought treatment caused a drop in average SAT for all hybrids except the GRC4, GRC5, and GRC8 (Table S6).

After recovery, an increase in average R_{Green} and R_{Red} and a decrease in R_{Blue} was observed. Additionally,
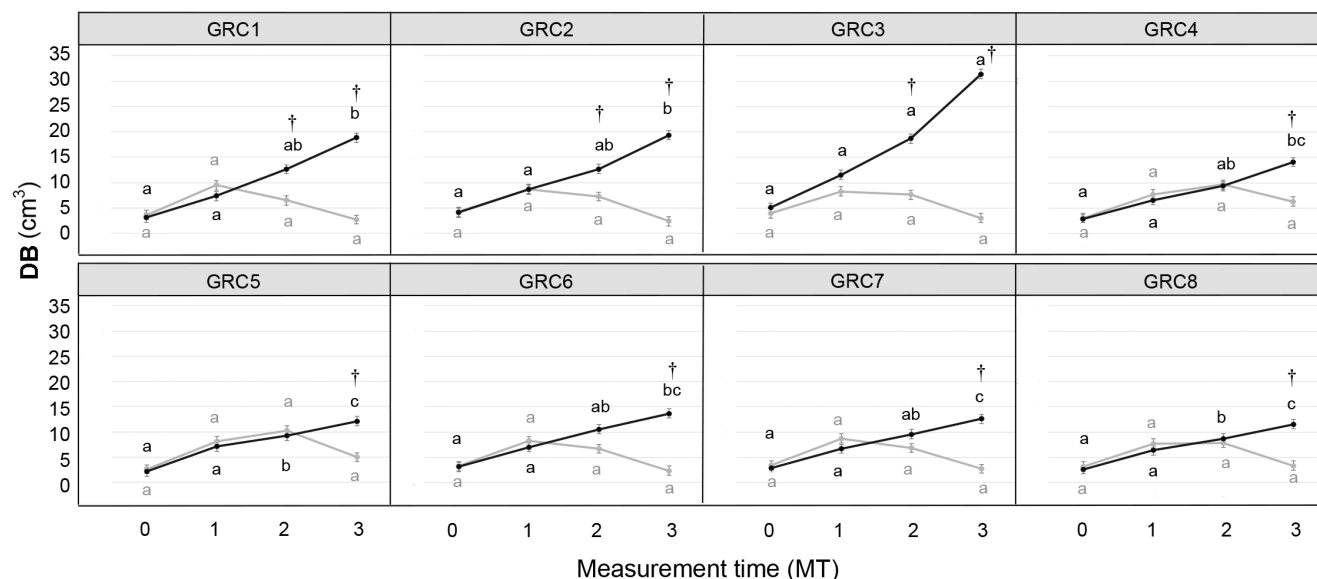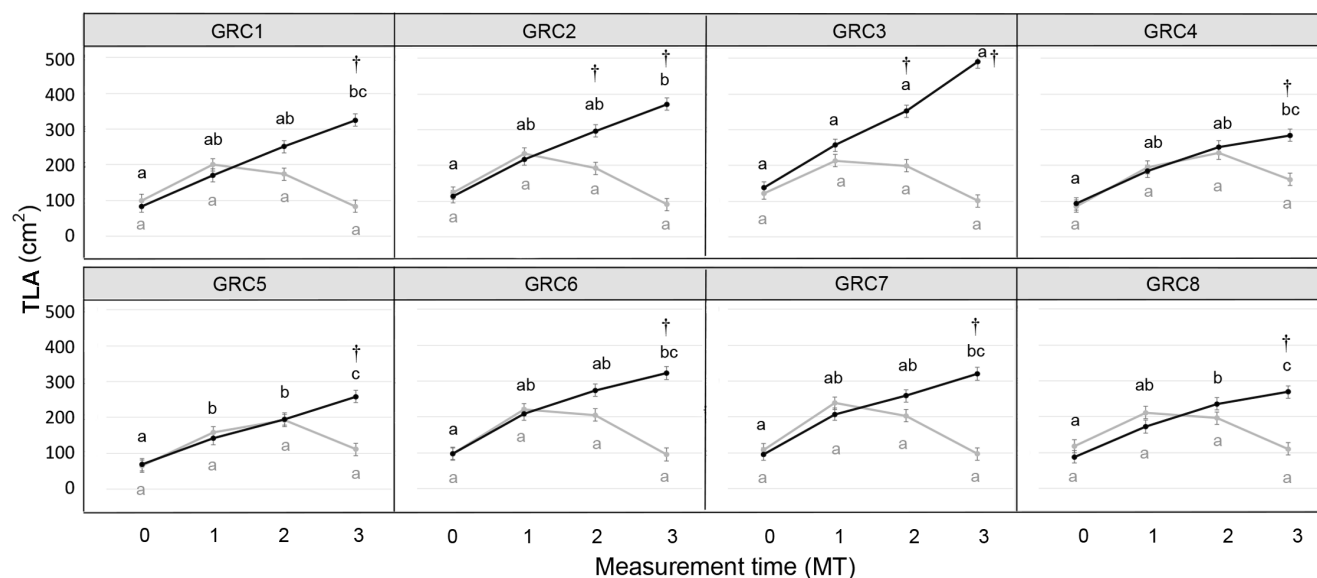
FIGURE 1 Digital biomass (DB) means and their standard error, measured at four measurement times—0 (MT0), 7 (MT1), 14 (MT2), and 21 (MT3) days after the onset of treatments—on eight *Miscanthus sinensis* hybrids (GRC1–GRC8) grown in control (black) and drought treatment (gray). Lowercase letters indicate significant differences among hybrids at each measurement time per treatment (black: control, gray: drought), dagger indicates significant difference between treatments within one timepoint for each hybrid (Tukey's HSD test).

FIGURE 2 Total leaf area (TLA) means and their standard error, measured at four measurement times—0 (MT0), 7 (MT1), 14 (MT2), and 21 (MT3) days after the onset of treatments—on eight *M. sinensis* hybrids (GRC1–GRC8) grown in control (black symbols) and drought treatment (gray symbols). Lowercase letters indicate significant differences among hybrids at each measurement time per treatment (black: control, gray: drought), dagger indicates significant difference between treatments for each hybrid at a single timepoint (Tukey's HSD test).

a significant increase in VAL was calculated for all hybrids. Similarly, an increment in SAT for all hybrids was reported, except for GRC5. Recovery did not affect average HUE, for which differences were found only among hybrids, with the highest found for GRC5 and lowest for GRC2 and GRC3 (Figure 5; Table S7).

4.3 | Multispectral traits and VIs during drought and recovery

Along with reflectance in the red, green, and blue spectrum, NIR and far-red reflectance (R_{NIR} and R_{FarRed}) were performed and used to calculate different VIs (NDVI, GR,
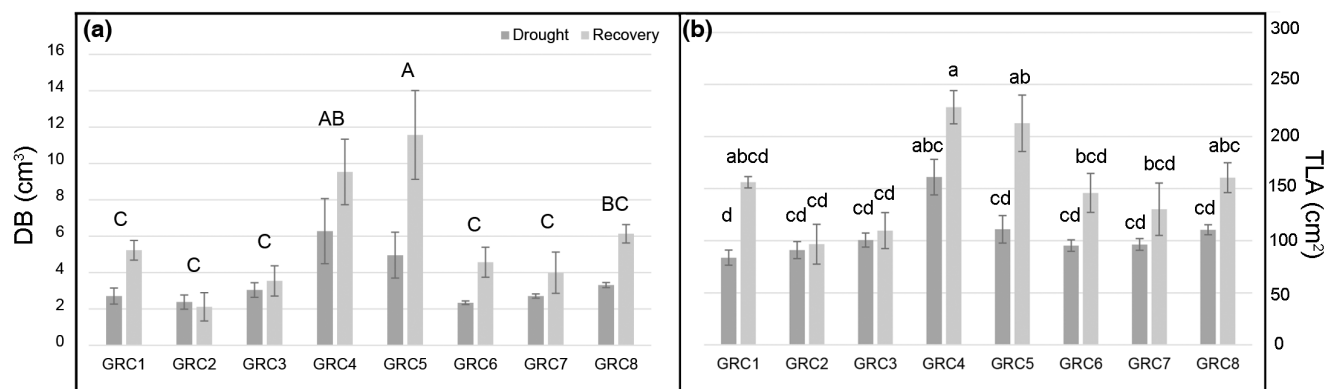
FIGURE 3 Means and their respective standard error for (a) digital biomass (DB) and (b) total leaf area (TLA), measured during drought (21 days without irrigation) and after the recovery (7 days of recovery) on eight *Miscanthus sinensis* hybrids (GRC1–GRC8). Different uppercase letters indicate significant differences among average values of hybrids; different lowercase letters indicate significant differences for hybrid × treatment interaction (Tukey's HSD test).
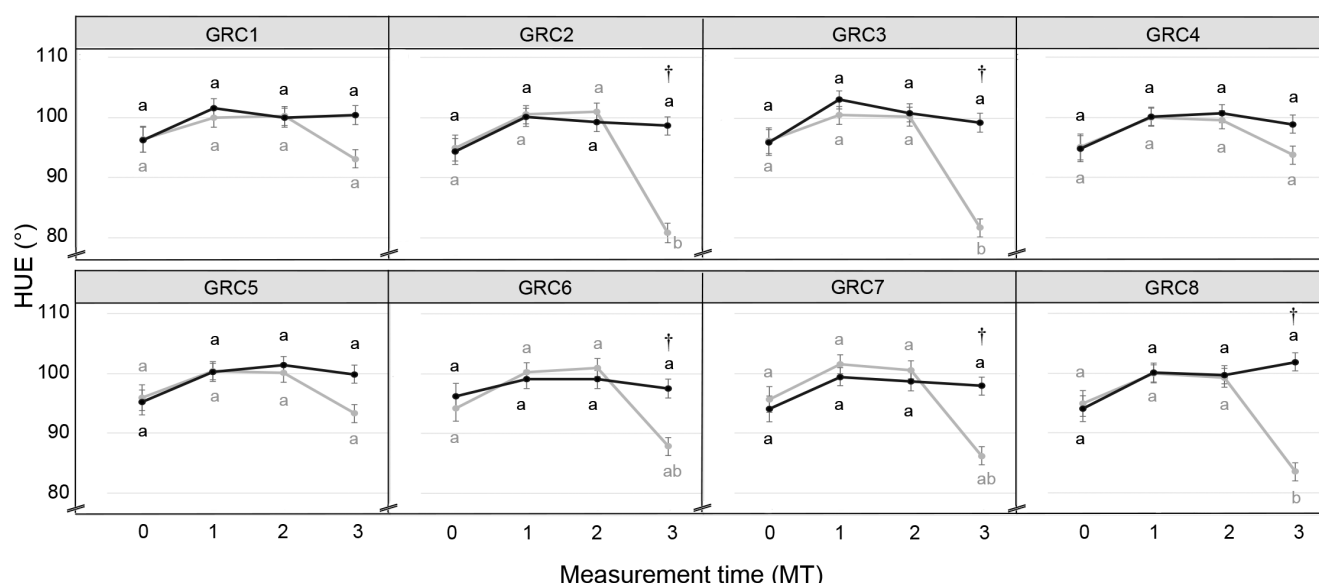

FIGURE 4 Hue (HUE) means and standard error of the mean, measured at four measurement times (0 (MT0), 7 (MT1), 14 (MT2), and 21 (MT3) days after the onset of treatments) on eight *Miscanthus sinensis* hybrids (GRC1–GRC8) grown in control (black symbols) and drought treatment (gray symbols). Lowercase letters indicate significant differences among hybrids at each measurement time for each treatment (black: control, gray: drought), dagger indicates measurement time at which significant difference between treatments for each hybrid occurred (Tukey's HSD test).

CHI, ARI, and PSRI). Drought significantly affected R_{NIR}, R_{FarRed}, as well as all VIs (Table S5). Earliest affected traits by drought were GR, NDVI, and R_{FarRed} for which a significant average decrease was reported at MT2, whereas for all other multispectral traits this was true only after 3 weeks of stress (MT3). The least affected hybrids regarding drought-caused changes in multispectral traits were GRC4 and GRC5. Namely, drought treatment significantly decreased only GR for GRC4 and GR, R_{NIR}, and NDVI for GRC5 (Table S6; Figure 6).

Earliest differences between C and D plants were determined at MT2 in NDVI and GR for GRC2 and R_{NIR} for GRC1 (Table S6). Moreover, ARI and CHI increased

from MT0 to MT1 for all plants but remained stable only in control plants for these traits in the subsequent measurements. At MT3 significant differences between C and D plants were found for GRC1, GRC2, GRC3 in ARI, and for GRC1, GRC2, GRC3, and GR8 in CHI, respectively (Figure 7; Table S6).

PSRI decreased for both C and D plants at MT1 compared with MT0 and was stable for C plants during subsequent measurements, while it recorded a significant increase in D plants at MT3 (Table S6).

After the recovery, a significant increase in average R_{NIR}, R_{FarRed}, NDVI, and GR across all hybrids was found. Significant differences in the average values of all

multispectral traits except R_{FarRed} were found among hybrids. Figure 8 shows these differences for NDVI and CHI. Additionally, a significant increase in PSRI for GRC2 and GRC3 was found (Table S7).

4.4 | Chlorophyll fluorescence during drought and recovery

Significant *measurement time × hybrid × treatment* interaction was found for $F_{\mathrm{v}}/F_{\mathrm{m}}$ (Table S5). $F_{\mathrm{v}}/F_{\mathrm{m}}$ values were constant across all measurement timepoints for control
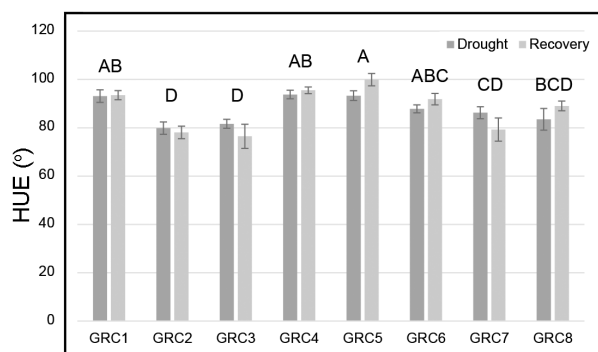
FIGURE 5 Hue (HUE) means and standard error of the mean, measured during drought (21 days without irrigation) and after the recovery (7 days) on eight *Miscanthus sinensis* hybrids (GRC1–GRC8). Different uppercase letters indicate significant differences among hybrids (Tukey's HSD test) after recovery.

plants. It, however, decreased significantly under stress after 3 weeks (MT3) for all hybrids except the GRC4 (Figure 9; Table S6). Conversely, $F_{\mathrm{v}}/F_{\mathrm{m}}$ increased when irrigation was reinstated for 7 days (Figure 10; Table S7).

4.5 | Phenotypic plasticity of the *M. sinensis* hybrids subjected to drought

Significant differences among eight *M. sinensis* hybrids were found for all examined phenotypic traits except R_{Green} and VAL (Table S8). In general, the highest average RDPIs were found for morphological traits DB, TLA, LAP, and LAI, and PSRI (Table S8). Most of the traits' highest RDPIs were found in GRC2 and GRC3, and lowest in GRC4, GRC5, and GRC8 (Figure 11; Table S8).

4.6 | The relationship among phenotypic traits

The relationships among measured traits on eight examined *M. sinensis* hybrids were tested by Pearson's correlation coefficients for drought and control treatment at MT3 (Figures S9a and S9b). Strong positive (>0.7) correlations in unstressed plants (C) were found among F_0, F_{m}, R_{FarRed}, and R_{NIR}, among R_{Red}, R_{Blue}, R_{Green}, VAL, R_{FarRed}, and among DB, TLA, LAP, and LPD. In addition, strong positive correlations were also found between CHI and
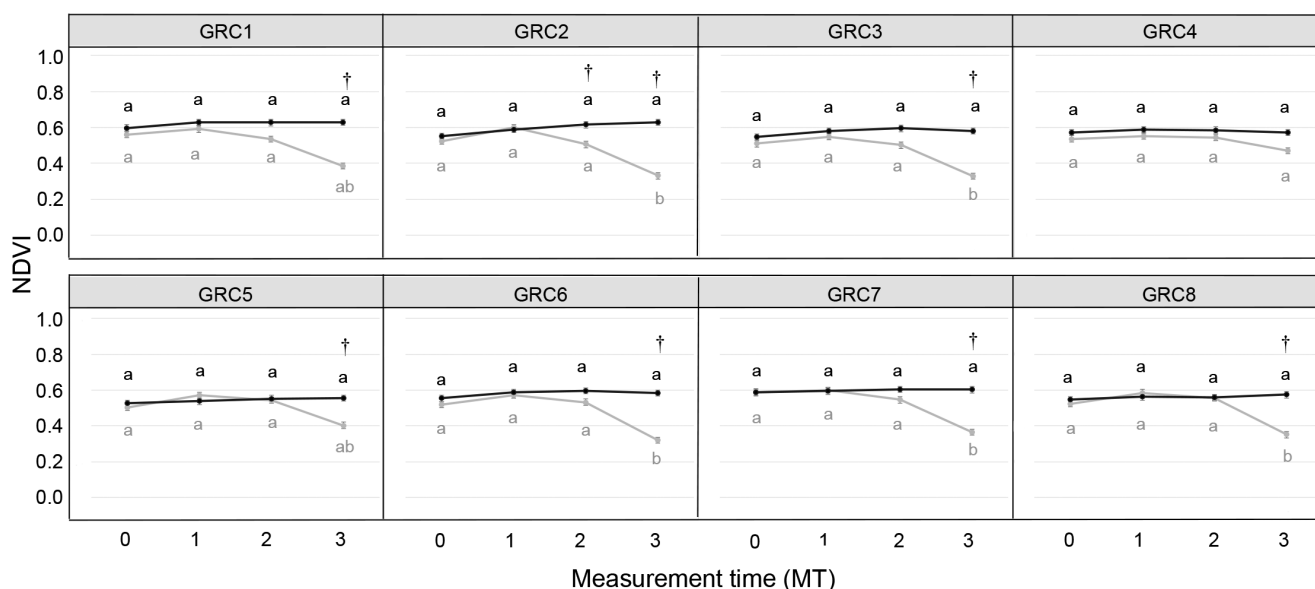

FIGURE 6 Normalized Difference Vegetation Index (NDVI) means and standard error of the mean, measured at four measurement times (0 (MT0), 7 (MT1), 14 (MT2), and 21 (MT3) days after the onset of treatments) on eight *Miscanthus sinensis* hybrids (GRC1–GRC8) grown in control (black symbols) and drought treatment (gray symbols). Lowercase letters indicate significant differences among hybrids at each measurement time for each treatment (black: control, gray: drought), dagger indicates measurement time at which a significant difference between treatments for each hybrid occurred (Tukey's HSD test).
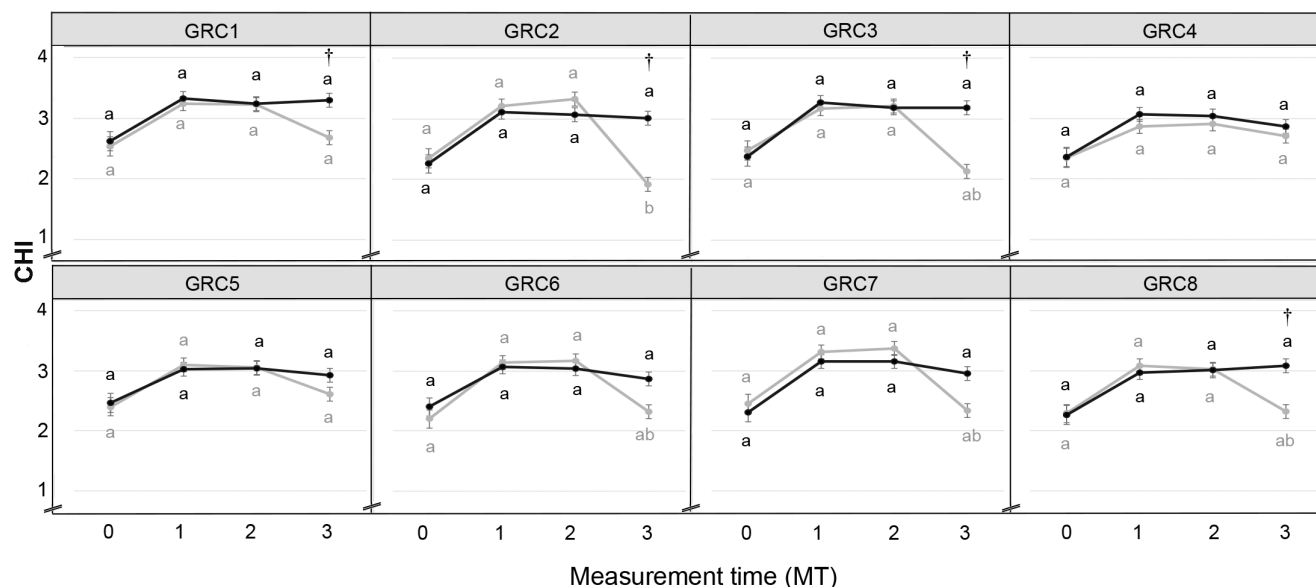
FIGURE 7 Chlorophyll Index (CHI) means and standard error of the mean, measured at four measurement times—0 (MT0), 7 (MT1), 14 (MT2), and 21 (MT3) days after the onset of treatments—on eight *Miscanthus sinensis* hybrids (GRC1–GRC8) grown in control (black symbols) and drought treatment (gray symbols). Lowercase letters indicate significant differences among hybrids at each measurement time for each treatment (black: control, gray: drought), dagger indicates measurement time at which significant difference between treatments for each hybrid occurred (Tukey's HSD test).
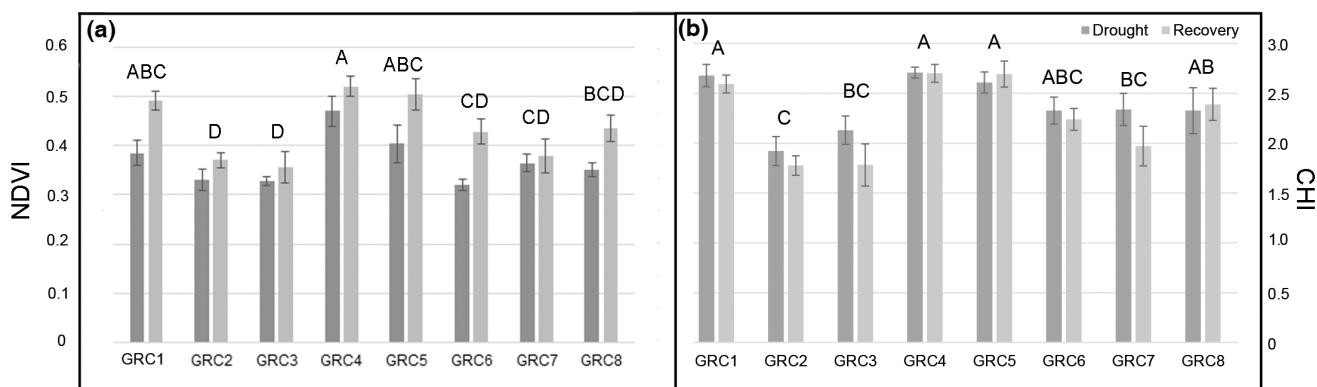

FIGURE 8 Means and standard error of the mean for (a) Normalized Difference Vegetation Index (NDVI) and (b) chlorophyll index (CHI), measured during drought (21 days without irrigation) and after the recovery (7 days of recovery) on eight *Miscanthus sinensis* hybrids (GRC1–GRC8). Different uppercase letters indicate significant differences among hybrids (Tukey's HSD test).

ARI, CHI and NDVI, NDVI, and GR, and between R_{NIR} and PH. Strong negative (<-0.7) correlations in the control treatment were found between F_v/F_m and R_{Green}, VAL, and R_{FarRed}, between CHI and R_{Red}, VAL, and R_{Green} and between HUE and VAL, and R_{Green} (Figure S9a). In drought stress, strong positive correlations were found among F_v/F_m and F_m, HUE, R_{NIR}, CHI, ARI, GR, and NDVI, among DB and PH, LANG, TLA, LAP, LPD, and NDVI, and among R_{Red}, R_{Green}, R_{Blue}, R_{FarRed}, and PSRI. In addition, strong negative correlations were found between LINC and F_v/F_m, R_{NIR}, HUE, GR, NDVI, and LANG,

between R_{Red} and HUE, CHI and ARI, and between PSRI and CHI and HUE (Figure S9b).

To identify traits which are the most responsive to drought, a PCA was performed. This analysis included all measured traits for all treatments and all plants at MT3 (Figure 12). The first two PCs had an eigenvalue higher than 1, and together explained 85.4% of the variation. The first component differentiated between treatments and was negatively correlated with LINC, R_{Blue}, and PSRI, whereas the strongest positive correlation was observed for F_m, R_{NIR}, NDVI, GR, LANG, LAP,
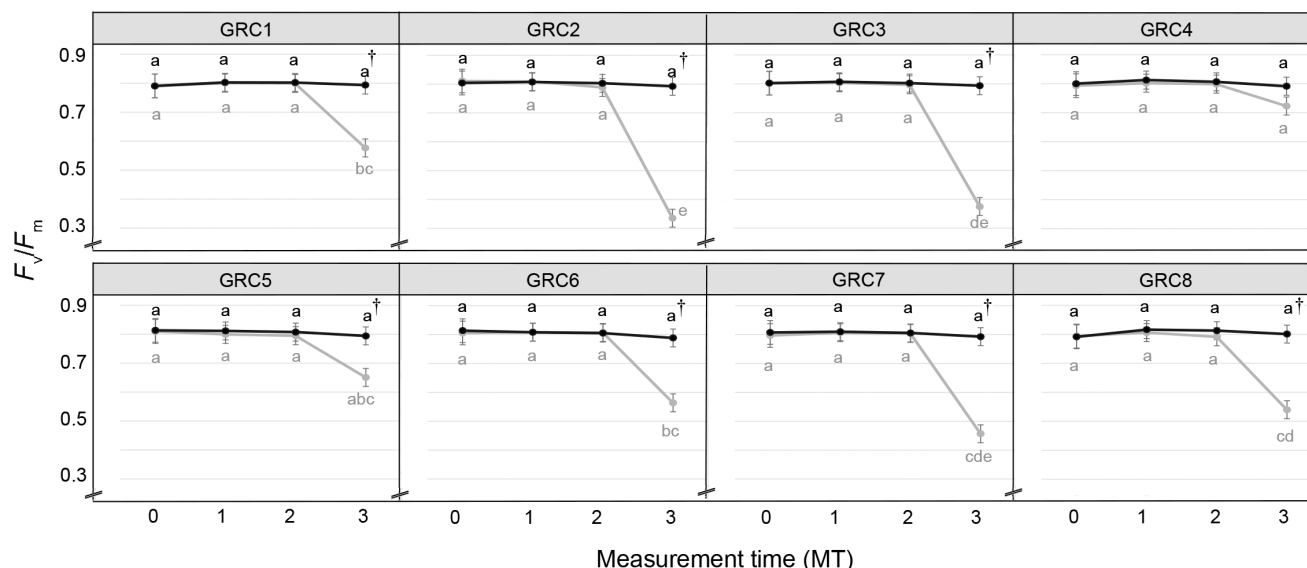
FIGURE 9 The maximum quantum yield of PSII (F_v/F_m) means, and standard error of the mean measured at four measurement times—0 (MT0), 7 (MT1), 14 (MT2), and 21 (MT3) days after the onset of treatments—on eight *Miscanthus sinensis* hybrids (GRC1–GRC8) grown in control (black symbols) and drought treatment (gray symbols). Lower case letters indicate significant differences among hybrids at each measurement time for each treatment (black: control, gray: drought), dagger indicates measurement time at which significant difference between treatments for each hybrid occurred (Tukey's HSD test).
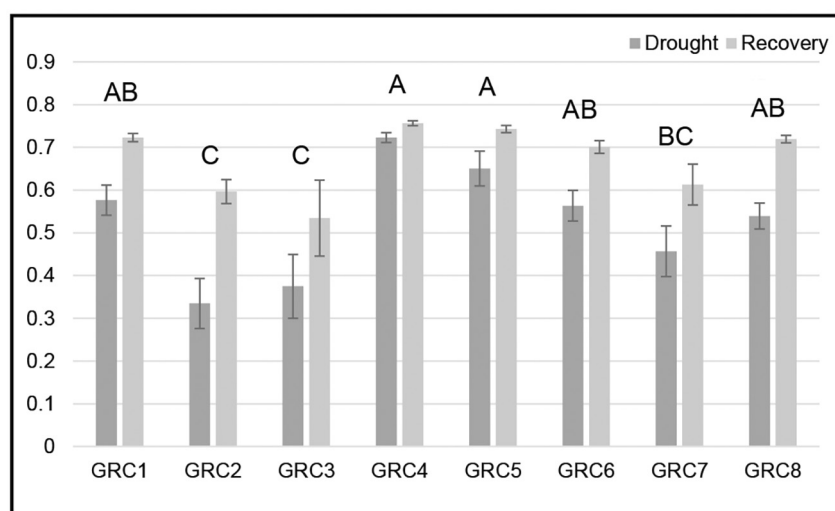

FIGURE 10 The maximum quantum yield of PSII (F_v/F_m) means and standard error of the mean measured during drought (21 days without irrigation). After the recovery (7 days of recovery) on eight *Miscanthus sinensis* hybrids (GRC1–GRC8). Different uppercase letters indicate significant differences among hybrids (Tukey's HSD test).

F_v/F_m, and TLA. The second PC (PC2) was more related to hybrid-specific differences, and was positively correlated with VAL, R_{Red}, and R_{Green}, and negatively with ARI, HUE, and CHI.

5 | DISCUSSION

Drought is considered as one of the most deleterious environmental stresses, radically impacting the yield of major crops (Cattivelli et al., 2008), and whose frequency and occurrence are forecasted to increase in the near future (Salinger et al., 2005). It is one of the major causes of marginality, notably in Europe (Von Cossel et al., 2019),

and its impact is critical, especially for low-input crop production such as biomass production on marginal land (Williams et al., 2014). An earlier detection of stress, and a better screening for susceptibility among industrial crops, would help mitigate and better prepare for this abiotic stress. In this study, we used a multispectral imaging and 3D scanning, and chlorophyll fluorescence imaging to monitor the physiological and morphological responses of different *M. sinensis* hybrids under drought conditions. A strategy that could prove vital in prescreening for drought tolerance and susceptibility, as well as identifying the responses to this stress in *M. sinensis*.

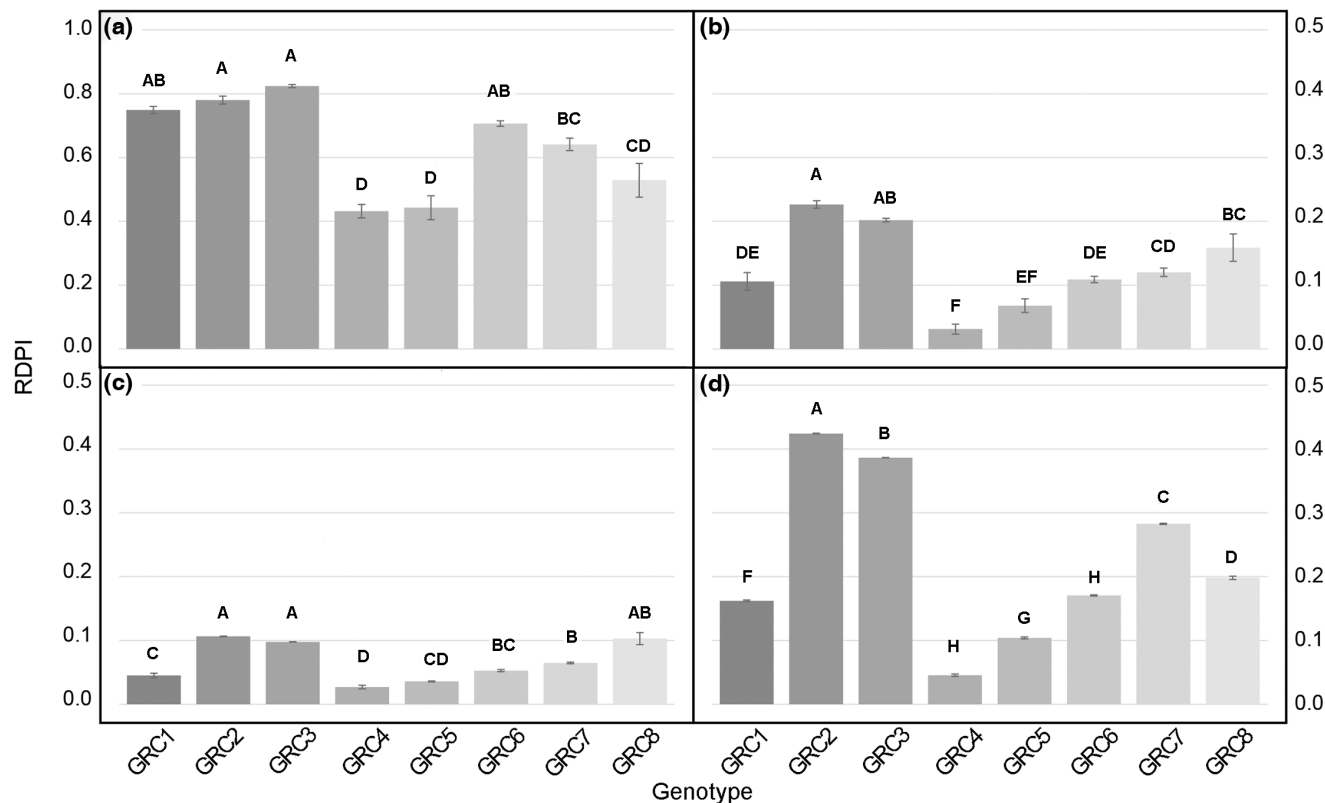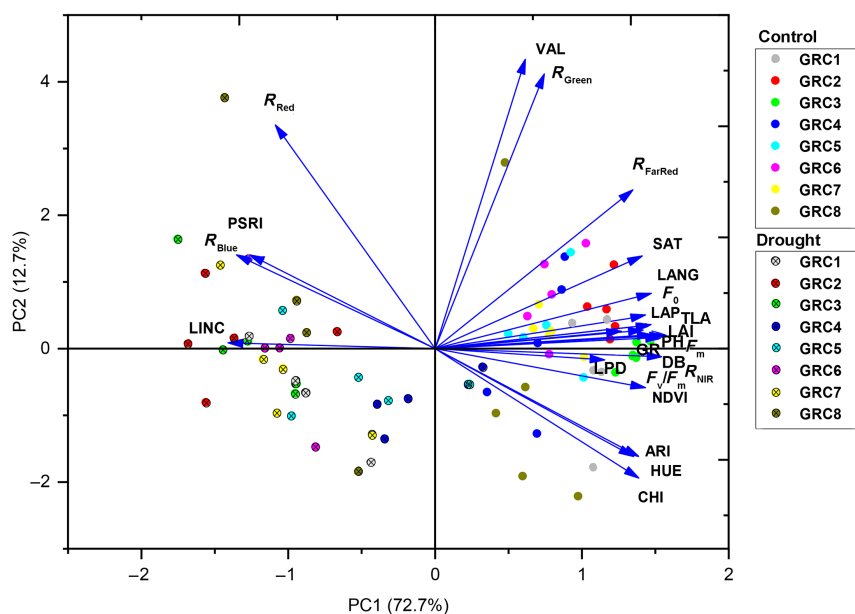Analysis of the morphological traits, obtained from 3D scans, revealed that drought has led to a significant

FIGURE 11 Relative distance plasticity index (RDPI) for (a) digital biomass (DB), (b) chlorophyll index (CHI), (c) hue (HUE), and (d) maximum quantum yield of PSII (F_v/F_m) in eight *Miscanthus sinensis* hybrids subjected to drought for 21 days (MT3). Different uppercase letters indicate significant differences among hybrids for each trait (Tukey's HSD test).

FIGURE 12 Biplot of principal component analysis based on 24 traits of eight *Miscanthus sinensis* hybrids (GRC1–GRC8) from two treatments [open circles: control, crossed circles: drought] measured at the third measurement time (MT3, 21 days after the onset of treatments).

decrease in all measured morphological traits, except the LINC, which increased. The earliest and the most pronounced reduction was obtained for DB and traits related to leaf area (LAP, TLA, and LAI). Reduction in plant biomass and leaf area is a typical plant response to drought (Farooq et al., 2009), which reduces metabolite

requirements (Chaves et al., 2003) and play an essential role in the regulation of heat dissipation and transpiration (Blum, 2005; Bridge et al., 2013). Similar drought-induced reduction in biomass and leaf area was previously described in Miscanthus (Al Hassan et al., 2022; Ings et al., 2013; Malinowska et al., 2017; van der Weijde

et al., 2017). However, the obtained drought-induced reduction in DB and leaf area traits were different among the examined hybrids, indicating a potential difference in response to drought. Namely, the most pronounced effect of drought on DB, TLA, LAP, and LAI reduction was reported in GRC1, GRC2, and GRC3, whereas those traits showed a smaller decrease in GRC4 and GRC5 (compared with their respective controls). Although nonsignificant, GRC4, and GRC5 achieved slightly higher DB, TLA, LAP, and LAI compared with other hybrids under drought. In the control treatment, those hybrids produced less DB, TLA, LAP, and LAI, only compared with GRC3. Similarly, van der Weijde et al. (2017) found that genotypes, which produce smaller biomass were less affected by drought compared with those with large biomass, which is in agreement with the expected tradeoff between growth vigor in favorable conditions and tolerance under stress (Bazzaz, 1996). This could explain *M. sinensis* better avoidance of drought compared with *M. × giganteus* and *M. sacchariflorus* (Clifton-Brown & Lewandowski, 2000), whereas the latter two accumulated higher biomass under control conditions. These findings concur with VWC (%) measurements made in this study. At MT2 (14 days of drought) GRC4 and GRC5 had 18.6% and 17.9% VWC, whereas the highest yielding hybrid, GRC3 had 9.4%. Although, the root biomass and morphology were not monitored for this work, root traits are essential for the water uptake from the soil (Lynch, 2018); in addition to differences in the above-ground biomass, hybrids with large root systems could be more efficient in water uptake from the pots, might deplete all available water at an earlier stage, and thus be subjected to drought stress for a longer period. However, in the field conditions, especially where water is supplied from the subsoil reserves, hybrids with larger (more in-depth) root systems could be less affected by drought. Therefore, any observations of superior traits for growing and surviving water deficits made in pots should be confirmed in field trials. Moreover, experiments conducted in the growing chambers often has limited light intensity (300 μmol m^{-2} s^{-1} in our experiment) which is much lower compared with field conditions and can have effect on the pigment synthesis as well as on photosynthetic performance.

Color analyses showed increased R_{Red}, R_{Blue}, and decreased HUE, SAT and VAL, which indicates changes in the pigment content and accelerated senescence of plants subjected to drought. This is further supported by the significant negative correlation between R_{Red} and R_{Blue} with VIs related to chlorophyll content (CHI, GR, and NDVI) and positive correlation with PSRI, for stressed plants. Higher PSRI indicates increased relative content of carotenoids compared with chlorophylls (Merzlyak et al., 1999). In summary, drought treatment led to a significant decrease in CHI, GR, and NDVI, and an increase in PSRI, R_{Red}, and R_{Blue}, which indicates a decrease in photosynthetic pigments, lower light absorption and an increase in yellow and brown pigments, a typical shift for senescing leaves (Li et al., 2014; Merzlyak et al., 2003; Mulla, 2013; Peñuelas & Filella, 1998). Moreover, decrease in R_{NIR} and GR under drought and their increase after the recovery are probably related to the plant water content. Peñuelas and Filella (1998) stated that there is a strong correlation between greenness and plant moisture content. As for the morphological traits, drought differently affected color, multispectral traits and VIs among examined hybrids with the earliest and the most profound effect found in GRC2 and GRC3; the least affected hybrids were found to be GRC4 and GRC5. Clifton-Brown and Lewandowski (2000) found that drought stress enhanced leaf senescence in *M. × giganteus* and *M. sacchariflorus*, whereas a selected *M. sinensis* genotype was less affected by drought and displayed a stay-green strategy. Malinowska et al. (2017) reported genotypic differences among *M. sinensis* genotypes in leaf senescence and stay-green strategy during short-term (5 weeks) water deficits. Similarly, for the most hybrids in this study, an average PSRI increased and CHI, GR and NDVI decreased at MT3, that is only after prolonged and severe drought.

In addition to the pigments related to photosynthesis, drought stress has affected the anthocyanin content as well. Gitelson et al. (2001) found that the concentration of anthocyanin as a photoprotective pigment increases under stressful conditions, whereas Feild et al. (2001) stated that their accumulation in senescing leaves enables nutrient remobilization. However, the results of this study show that drought treatment has decreased the average ARI; a significant reduction in ARI was found in GRC1, GRC2, GRC3, and GRC8 at MT3. This could be explained by the fact that under the drought treatment at MT3, most of the leaves were already dead and had low reflectance, whereas newly developed young leaves in control plants contained high anthocyanin levels, which are noticeable on control plants shown in Figure S3.

Results of the chlorophyll fluorescence imaging showed that the maximum efficiency of PSII (F_v/F_m) decreases only after a prolonged and severe water-deficiency stress and was more affected by the decrease in F_m. Although it is one of the most widely used physiological parameters for estimating plant performance under stressful conditions, many authors have reported that F_v/F_m is not sensitive to an early or moderate water stress (Bukhov & Carpentier, 2004; Massacci et al., 2008). Bresson et al. (2015) found that under drought conditions, *Arabidopsis thaliana* show bimodal F_v/F_m distribution with regions showing high and low F_v/F_m, respectively, while plants retain stable average F_v/F_m values over a

prolonged period. In the presented work, differences were found among investigated *M. sinensis* hybrids where the highest F_v/F_m values in drought treatment were reported for GRC4 and GRC5, and the lowest for GRC2 and GRC3. After recovery all hybrids show increase in F_v/F_m; however, there were significant differences among studied hybrids. Moreover, average F_v/F_m values were below 0.74 indicating damaged photosystems. Thus, although F_v/F_m is not considered as good indicator of drought tolerance, it could be more useful as an indicator of plant recovery from drought.

Traits that renormalized the best in the early post-stress recovery, were DB, TLA, LAP, LAI, F_m, and GR. Several traits, such as PH, LPD, LANG, LINC, HUE, CHI, and ARI did not significantly change, whereas PSRI continued to increase during the recovery period, probably not only due to an ongoing senescence of surviving leaves after drought treatment but also due to new leaf development, which also show higher PSRI value. After the recovery, GRC4 and GRC5 showed the highest DB, PH, LAP, LAI, TLA, F_v/F_m, HUE, R_{NIR}, GR, ARI, CHI, and NDVI, but the lowest values in PSRI, for their recovering plants, compared with other hybrids, which indicates the fastest response of these hybrids to more favorable conditions. This is enabled by a smaller disruption of homeostasis under stress (Al Hassan et al., 2022).

To identify traits which are most responsive to drought stress, a PCAs was performed. PC1 corresponds to differences among the treatments and explained 72.7% of the total variation. The highest positive contribution to PC1 was found for F_m, R_{NIR}, NDVI, GR, LANG, LAP, F_v/F_m, and TLA, whereas the highest negative contribution was found for LINC, R_{Blue}, and PSRI. The latter indicates an enhanced plant senescence and withering in the prolonged drought treatment. The fact that GRC4 drought-treated plants have similar PC1 scores to the control plants indicates a stay-green strategy for this hybrid. Due to a large number of examined traits, a phenotypic plasticity (RDPI) was calculated to have more comparable data on the performance of different hybrids under the drought treatment. In general, a higher phenotypic plasticity was found for the morphological traits compared with physiological traits, indicating the plant strategy to reduce water usage, metabolic costs and sustain metabolic activity under drought. The effect of biomass and leaf area reductions, as a strategy, which reduces transpiration and protects photosynthesis from the negative impact of water deficit, has already been described and discussed (Blum, 2005; Bridge et al., 2013; Chaves et al., 2003). Although it is suggested that the plant growth in adverse environments can benefit from the plasticity in some functional traits (Matesanz et al., 2010), drought-sensitive hybrids (such as GRC2 and

GRC3) in this study have shown the highest RDPI for most of the examined traits, whereas the most tolerant hybrids (GRC4 and GRC5) showed the lowest RDPI, respectively. Similarly, Marchiori et al. (2017) found higher RDPI for morphological traits in drought susceptible compared with drought-tolerant sugarcane (*Saccharum* spp.). Alpert and Simms (2002) explained such plasticity phenomenon as "injurious plasticity" or inability to compensate for environmental stress.

6 | CONCLUSION

The employed phenotyping techniques enabled a nondestructive study of morphophysiological traits in *M. sinensis* hybrids during drought and recovery. The earliest and most affected traits by drought were related to the reduction in leaf area and DB, followed by enhanced leaf senescence, and finally, a drop in the maximum efficiency of PSII. Significant differences in drought avoidance were found among the studied hybrids, indicating their potential for optimized drought tolerance through breeding, and possible application in biomass production in drought-prone environments. Drought-resilient hybrids showed lower phenotypic plasticity compared with their relatively more sensitive counterparts, with smaller biomass reduction under drought and a stay-green strategy. Combining remote sensing phenotyping techniques with gas exchange measurements and root architecture analysis, and validation of this results under field conditions would provide a more comprehensive insight in *M. sinensis* performance under drought conditions. Moreover, in combination with advanced genetic studies, these techniques could be used in breeding programs to screen for genes related to drought tolerance.

AUTHOR CONTRIBUTIONS

Boris Lazarević and Mislav Kontek designed the study and performed the measurements. Vanja Jurišić and Klaudija Carović-Stanko were involved in planning and supervised the work. Luisa M. Trindade and Mohamad Al Hassan provided plant materials. Boris Lazarević and Mislav Kontek processed the experimental data, performed the data analysis, and drafted the manuscript. Vanja Jurišić, Klaudija Carović-Stanko, John Clifton-Brown, Mohamad Al Hassan, and Luisa M. Trindade contributed to the final version of the manuscript, by aiding in result interpretation and working on the manuscript. All authors discussed the results and contributed to the final manuscript.

CONFLICT OF INTEREST

The authors declare no conflict of interest.

ORCID

Boris Lazarević https://orcid.org/0000-0002-2521-7500
Mislav Kontek https://orcid.org/0000-0001-9042-5499
Klaudija Carović-Stanko https://orcid.org/0000-0002-8777-9875
John Clifton-Brown https://orcid.org/0000-0001-6477-5452
Mohamad Al Hassan https://orcid.org/0000-0002-2297-3394
Luisa M. Trindade https://orcid.org/0000-0003-1541-2094
Vanja Jurišić https://orcid.org/0000-0002-4071-8637

REFERENCES

Al Hassan, M., van der Cruijsen, K., Dees, D., Dolstra, O., & Trindade, L. M. (2022). Investigating applied drought in *Miscanthus sinensis*; sensitivity, response mechanisms, and subsequent recovery. *GCB Bioenergy*, *14*, 756–775. https://doi.org/10.1111/gcbb.12941

Alpert, P., & Simms, E. L. (2002). The relative advantages of plasticity and fixity in different environments: When is it good for a plant to adjust? *Evolutionary Ecology*, *16*, 285–297. https://doi.org/10.1023/A:1019684612767

Bazzaz F. A. (1996). *Plants in changing environments: Linking physiological, population, and community ecology*. Cambridge University Press. ISBN:0521391903.

Blum, A. (2005). Drought resistance, water-use efficiency, and yield potential—Are they compatible, dissonant, or mutually exclusive? *Australian Journal of Agricultural Research*, *56*, 1159–1168. https://doi.org/10.1071/AR05069

Bresson, J., Vasseur, F., Dauzat, M., Koch, G., Granier, C., & Vile, D. (2015). Quantifying spatial heterogeneity of chlorophyll fluorescence during plant growth and in response to water stress. *Plant Methods*, *11*(1), 1–15. https://doi.org/10.1186/s13007-015-0067-5

Bridge, L. J., Franklin, K. A., & Homer, M. E. (2013). Impact of plant shoot architecture on leaf cooling: A coupled heat and mass transfer model. *Journal of the Royal Society Interface*, *10*(85), 20130326. https://doi.org/10.1098/rsif.2013.0326

Bukhov, N. G., & Carpentier, R. (2004). Effects of water stress on the photosynthetic efficiency of plants. In G. C. Papageorgiou & R.

Govindjee (Eds.), *Chlorophyll a fluorescence. Advances in photosynthesis and respiration* (pp. 623–635). Springer, Netherlands. https://doi.org/10.1007/978-1-4020-3218-9_24

Cattivelli, L., Rizzaa, F., Badeck, F. W., Mazzucotelli, E., Mastrangelo, A. M., Francia, E., Marè, C., Tondelli, A., & MicheleStanca, A. (2008). Drought tolerance improvement in crop plants: An integrated view from breeding to genomics. *Field Crops Research*, *105*, 1–14. https://doi.org/10.1016/j.fcr.2007.07.004

Chaves, M. M., Maroco, J. P., & Pereira, J. S. (2003). Understanding plant responses to drought – From genes to the whole plant. *Functional Plant Biology*, *30*, 239–264. https://doi.org/10.1071/FP02076

Clifton-Brown, J., Hastings, A., Mos, M., McCalmont, J. P., Ashman, C., Awty-Carroll, D., Cerazy, J., Chiang, Y. C., Cosentino, S., Cracroft-Eley, W., Scurlock, J., Donnison, I. S., Glover, C., Gołąb, I., Greef, J. M., Gwyn, J., Harding, G., Hayes, C., Helios, W., … Flavell, R. (2017). Progress in upscaling Miscanthus biomass production for the European bio-economy with seed-based genotypes. *GCB Bioenergy*, *9*(1), 6–17. https://doi.org/10.1111/gcbb.12357

Clifton-Brown, J., & Lewandowski, I. (2000). Water use efficiency and biomass partitioning of three different Miscanthus genotypes with limited and unlimited water supply. *Annals of Botany*, *86*(1), 191–200. https://doi.org/10.1006/anbo.2000.1183

da Costa, R. M. F., Simister, R., Roberts, L. A., Timms-Taravella, E., Cambler, A. B., Corke, F. M. K., Han, J., Ward, R. J., Buckeridge, M. S., Gomez, L. D., & Bosch, M. (2019). Nutrient and drought stress: Implications for phenology and biomass quality in Miscanthus. *Annals of Botany*, *124*(4), 553–566. https://doi.org/10.1093/aob/mcy155

Dhondt, S., Wuyts, N., & Inze, D. (2013). Cell to whole-plant phenotyping: The best is yet to come. *Trends in Plant Science*, *18*, 433–444. https://doi.org/10.1016/J.Tplants.2013.04.008

Donnison, I. S., & Fraser, M. D. (2016). Diversification and use of bioenergy to maintain future grasslands. *Food and Energy Security*, *5*(2), 67–75. https://doi.org/10.1002/fes3.75

FAO. (2018). *The future of food and agriculture – Alternative pathways to 2050*. Food and Agriculture Organization of the United Nations Rome, 224 pp.

Farooq, M. A., Wahid, N., Kobayashi, N., Fujita, D. B., & Basra, S. M. (2009). Plant drought stress: Effects, mechanisms and management. In *Sustainable agriculture* (pp. 153–188). Springer. https://doi.org/10.1007/978-90-481-2666-8_12

Feild, T. S., Lee, D. W., & Holbrook, N. M. (2001). Why leaves turn red in autumn. The role of anthocyanins in senescing leaves of red-osier dogwood. *Plant Physiology*, *127*, 566–574. https://doi.org/10.1104/pp.010063

Gauder, M., Graeff-Honninger, S., Lewandowski, I., & Claupein, W. (2012). Long-term yield and performance of 15 different *Miscanthus* genotypes in southwest Germany. *The Annals of Applied Biology*, *160*, 126–136. https://doi.org/10.1111/j.1744-7348.2011.00526.x

Gifford, J. M., Chae, W. B., Swaminathan, K., Moose, S. P., & Juvik, J. A. (2015). Mapping the genome of *Miscanthus sinensis* for QTL associated with biomass productivity. *GCB Bioenergy*, *7*, 797–810. https://doi.org/10.1111/gcbb.12201

Gitelson, A. A., Gritz, Y., & Merzlyak, M. N. (2003). Relationships between leaf chlorophyll content and spectral reflectance and algorithms for nondestructive chlorophyll assessment in higher

plant leaves. *Journal of Plant Physiology*, *160*(1), 271–282. https://doi.org/10.1078/0176-1617-00887

Gitelson, A. A., Merzlyak, M. N., & Chivkunova, O. B. (2001). Optical properties and nondestructive estimation of anthocyanin content in plant leaves. *Photochemistry and Photobiology*, *74*(1), 38–45. https://doi.org/10.1562/0031-8655(2001)0740038OPANEO2.0.CO2

Greef, J. M., & Deuter, M. (1993). Syntaxonomy of *Miscanthus × giganteus* GREEF et DEU. *Angewandte Botanik*, *67*, 87–90.

He, Y., Jaiswal, D., Liang, X.-Z., Sun, C., & Long, S. P. (2022). Perennial biomass crops on marginal land improve both regional climate and agricultural productivity. *GCB Bioenergy*, *14*, 558–571. https://doi.org/10.1111/gcbb.12937

Hoagland, D. R., & Arnon, D. I. (1950). The water-culture method for growing plants without soil. *Circular. California Agricultural Experiment Station*, *347*, 1–32.

Humplik, J. F., Lazar, D., Furst, T., Husickova, A., Hybl, M., & Spichal, L. (2015). Automated integrative high-throughput phenotyping of plant shoots: A case study of the cold-tolerance of pea (*Pisum sativum* L.). *Plant Methods*, *11*(1), 20. https://doi.org/10.1186/s13007-015-0063-9

Ings, J., Mur, L. A. J., Robson, P. R. H., & Bosch, M. (2013). Physiological and growth responses to water deficit in the bioenergy crop *Miscanthus × giganteus*. *Frontiers in Plant Science*, *4*, 468. https://doi.org/10.3389/fpls.2013.00468

Jones, M. B., Finnan, J., & Hodkinson, T. R. (2015). Morphological and physiological traits for higher biomass production in perennial rhizomatous grasses grown on marginal land. *GCB Bioenergy*, *7*(2), 375–385. https://doi.org/10.1111/gcbb.12203

Kalinina, O., Nunn, C., Sanderson, R., Hastings, A. F. S., van der Weijde, T., Özgüven, M., Tarakanov, I., Schüle, H., Trindade, L. M., Dolstra, O., Schwarz, K.-U., Iqbal, Y., Kiesel, A., Mos, M., Lewandowski, I., & Clifton-Brown, J. C. (2017). Extending miscanthus cultivation with novel germplasm at six contrasting sites. *Frontiers in Plant Science*, *8*, 563. https://doi.org/10.3389/fpls.2017.00563

Lazarević, B., Šatović, Z., Nimac, A., Vidak, M., Gunjača, J., Politeo, O., & Carović-Stanko, K. (2021). Application of phenotyping methods in detection of drought and salinity stress in basil (*Ocimum basilicum* L.). *Frontiers in Plant Science*, *12*, 629441. https://doi.org/10.3389/fpls.2021.629441

Lewandowski, I., Clifton-Brown, J., Kiesel, A., Hastings, A., & Iqbal, Y. (2018). Miscanthus. In E. Alexopoulou (Ed.), *Perennial grasses for bioenergy and bioproducts* (pp. 35–59). Academic Press. https://doi.org/10.1016/B978-0-12-812900-5.00002-3

Lewandowski, I., Clifton-Brown, J., Trindade, L. M., van der Linden, G., Schwarz, K. U., Müller-Sämann, K., Anisimov, A., Chen, C. L., Dolstra, O., Donnison, I. S., Farrar, K., Fonteyne, S., Harding, G., Hastings, A., Huxley, L. M., Iqbal, Y., Khokhlov, N., Kiesel, A., Lootens, P., … Kalinina, O. (2016). Progress on optimizing miscanthus biomass production for the European bioeconomy: Results of the EU FP7 project OPTIMISC. *Frontiers in Plant Science*, *7*, 1620. https://doi.org/10.3389/fpls.2016.01620

Lewandowski, I., & Schmidt, U. (2006). Nitrogen, energy and land use efficiencies of Miscanthus, reed canary grass and triticale as determined by the boundary line approach. *Agriculture, Ecosystems and Environment*, *112*(4), 335–346. https://doi.org/10.1016/j.agee.2005.08.003

Li, L., Zhang, Q., & Huang, D. (2014). A review of imaging techniques for plant phenotyping. *Sensors (Switzerland)*, *14*, 20078–20111. https://doi.org/10.3390/s141120078

Lynch, J. P. (2018). Rightsizing root phenotypes for drought resistance. *Journal of Experimental Botany*, *69*(13), 3279–3292. https://doi.org/10.1093/jxb/ery048

Malinowska, M., Donnison, I. S., & Robson, P. R. (2017). Phenomics analysis of drought responses in Miscanthus collected from different geographical locations. *GCB Bioenergy*, *9*, 78–91. https://doi.org/10.1111/gcbb.12350

Marchiori, P. E. R., Machado, E. C., Sales, C. R. G., Espinoza-Núñez, E., Magalhães Filho, J. R., Souza, G. M., Pires, R. C. M., & Ribeiro, R. V. (2017). Physiological plasticity is important for maintaining sugarcane growth under water deficit. *Frontiers in Plant Science*, *8*, 2148. https://doi.org/10.3389/fpls.2017.02148

Massacci, A., Nabiev, S. M., Pietrosanti, L., Nematov, S. K., Chernikova, T. N., Thor, K., & Leipner, J. (2008). Response of the photosynthetic apparatus of cotton (*Gossypium hirsutum*) to the onset of drought stress under field conditions studied by gas-exchange analysis and chlorophyll fluorescence imaging. *Plant Physiology and Biochemistry*, *46*, 189–195. https://doi.org/10.1016/j.plaphy.2007.10.006

Matesanz, S., Gianoli, E., & Valladares, F. (2010). Global change and the evolution of phenotypic plasticity in plants. *Annals of the New York Academy of Sciences*, *1206*, 35–55. https://doi.org/10.1111/j.1749-6632.2010.05704.x

Merzlyak, M. N., Gitelson, A. A., Chivkunova, O. B., & Rakitin, V. Y. (1999). Nondestructive optical detection of pigment changes during leaf senescence and fruit ripening. *Physiologia Plantarum*, *106*, 135–141. https://doi.org/10.1034/j.1399-3054.1999.106119.x

Merzlyak, M. N., Gitelson, A. A., Chivkunova, O. B., Solovchenko, A. E., & Pogosyan, S. I. (2003). Application of reflectance spectroscopy for analysis of higher plant pigments. *Russian Journal of Plant Physiology*, *50*, 704–710. https://doi.org/10.1023/A:1025608728405

Mulla, D. J. (2013). Twenty five years of remote sensing in precision agriculture: Key advances and remaining knowledge gaps. *Biosystems Engineering*, *114*, 358–371. https://doi.org/10.1016/j.biosystemseng.2012.08.009

Munns, R., James, R. A., Sirault, X. R., Furbank, R. T., & Jones, H. G. (2010). New phenotyping methods for screening wheat and barley for beneficial responses to water deficit. *Journal of Experimental Botany*, *61*, 3499–3507. https://doi.org/10.1093/jxb/erq199

Nie, G., Tang, L., Zhang, Y., Huang, L., Ma, X., Cao, X., Pan, L., Zhang, X., & Zhang, X. (2017). Development of SSR markers based on transcriptome sequencing and association analysis with drought tolerance in perennial grass miscanthus from China. *Frontiers in Plant Science*, *8*, 801. https://doi.org/10.3389/fpls.2017.00801

Osakabe, Y., Osakabe, K., Shinozaki, K., & Tran, L. S. (2014). Response of plants to water stress. *Frontiers in Plant Science*, *5*, 86. https://doi.org/10.3389/fpls.2014.00086

Peñuelas, J., & Filella, L. (1998). Visible and near-infrared reflectance techniques for diagnosing plant physiological status. *Trends in Plant Science*, *3*, 151–156. https://doi.org/10.1016/S1360-1385(98)01213-8

Quinn, L. D., Straker, K. C., Guo, J., Kim, S., Thapa, S., Kling, G., Lee, D. K., & Voigt, T. B. (2015). Stress-tolerant feedstocks for

sustainable bioenergy production on marginal land. *Bioenergy Research*, *8*, 1081–1100.

Rouse, J. W., Haas, R. H., Schell, J. A., Deering, D. W., & Harlan, J. C. (1974). *Monitoring the vernal advancement and retrogradation (green wave effect) of natural vegetation*. NASA/GSFC Type III Final Report, Greenbelt, MD.

Sacks, E. J., Juvik, J. A., Lin, Q., Stewart, J. R., & Yamada, T. (2013). The gene pool of *Miscanthus* species and its improvement. In A. H. Paterson (Ed.), *Genomics of the Saccharinae* (pp. 73–101). Springer.

Salinger, M. J., Sivakumar, M. V. K., & Motha, R. (2005). Reducing vulnerability of agriculture and forestry to climate variability and change: Workshop summary and recommendations. *Climatic Change*, *70*, 341–362. https://doi.org/10.1007/s10584-005-5954-8

Schreiber, U. B., Bilger, W., & Neubauer, C. (1995). Chlorophyll fluorescence as a nonintrusive indicator for rapid assessment of in vivo photosynthesis. In E. D. Schulze & M. M. Caldwell (Eds.), *Ecophysiology of photosynthesis* (pp. 49–70). Springer. https://doi.org/10.1007/978-3-642-79354-7_3

Scordia, D., Papazoglou, E. G., Kotoula, D., Sanz, M., Ciria, C. S., Pérez, J., Maliarenko, O., Prysiazhniuk, O., von Cossel, M., Greiner, B. E., Lazdina, D., Makovskis, K., Lamy, I., Ciadamidaro, L., Petit-dit-Grezeriat, L., Corinzia, S. A., Fernando, A. L., Alexopoulou, E., & Cosentino, S. L. (2022). Towards identifying industrial crop types and associated agronomies to improve biomass production from marginal lands in Europe. *GCB Bioenergy*, *14*, 710–734. https://doi.org/10.1111/gcbb.12935

Tuberosa, R. (2012). Phenotyping for drought tolerance of crops in the genomics era. *Frontiers in Physiology*, *3*, 347. https://doi.org/10.3389/fphys.2012.00347

Valladares, F., Sanchez-Gomez, D., & Zavala, M. A. (2006). Quantitative estimation of phenotypic plasticity: Bridging the gap between the evolutionary concept and its ecological applications. *Journal of Ecology*, *94*(6), 1103–1116. https://doi.org/10.1111/j.1365-2745.2006.01176.x

van der Weijde, T., Huxley, L. M., Hawkins, S., Sembiring, E. H., Farrar, K., Dolstra, O., Visser, G. F., & Trindade, L. M. (2017). Impact of drought stress on growth and quality of miscanthus for biofuel production. *GCB Bioenergy*, *9*, 770–782. https://doi.org/10.1111/gcbb.12382

Von Cossel, M., Wagner, M., Lask, J., Magenau, E., Bauerle, A., Warrach-Sagi, K., Elbersen, B., Staritsky, I., van Eupen, M., Iqbal, Y., Jablonowski, N. D., Happe, S., Fernando, A. L., Scordia, D., Cosentino, S. L., Wulfmeyer, V., Lewandowski, I., & Winkler, B. (2019). Prospects of bioenergy cropping systems for a more social-ecologically sound bioeconomy. *Agronomy*, *9*(10), 605. https://doi.org/10.3390/agronomy9100605

Wagner, M., Mangold, A., Lask, J., Petig, E., Kiesel, A., & Lewandowski, I. (2019). Economic and environmental performance of miscanthus cultivated on marginal land for biogas production. *GCB Bioenergy*, *11*(1), 34–49. https://doi.org/10.1111/gcbb.12567

Wang, H., Qian, X., Zhang, L., Xu, S., Li, H., Xia, X., Dai, L., Xu, L., Yu, J., & Liu, X. (2018). A method of high throughput monitoring crop physiology using chlorophyll fluorescence and multispectral imaging. *Frontiers in Plant Science*, *9*, 407. https://doi.org/10.3389/fpls.2018.00407

Williams, I. N., Torn, M. S., Riley, W. J., & Wehner, M. F. (2014). Impacts of climate extremes on gross primary production under global warming. *Environmental Research Letters*, *9*(9), 1–10. https://doi.org/10.1088/1748-9326/9/9/094011

SUPPORTING INFORMATION

Additional supporting information can be found online in the Supporting Information section at the end of this article.